

Reactions of the O^- Negative Ion with Hydrogen and the Lower Hydrocarbons

DAVID A. PARKES *

Chemistry Division, A.E.R.E., Harwell, Didcot, Berkshire

Received 8th October, 1971

The reactions between O^- , formed by dissociative attachment to oxygen, and H_2 , D_2 , CH_4 , C_2H_6 , C_2H_4 and C_2H_2 have been studied using a drift tube and mass filter. Gas densities ranged over a factor of five about 10^{17} molecule cm^{-3} and reduced fields were of the order of 3×10^{-16} V cm^2 molecule $^{-1}$. The reaction with the alkanes gave a single pair of products $R+OH^-$, but the remainder produced both negative ions and free electrons. The following rate constants were measured and with the minor exception of OH^- production from C_2H_4 were found to be substantially independent of the reduced field.

	$k/(cm^3 \text{ molecule}^{-1} s^{-1} \times 10^{-10})$
$O^- + H_2 = H_2O + e$	7.0 ± 0.5
$= OH^- + H$	0.33 ± 0.05
$O^- + D_2 = D_2O + e$	4.8 ± 0.5
$= OD^- + D$	0.1 ± 0.02
$O^- + CH_4 = OH^- + CH_3$	1.1 ± 0.1
$O^- + C_2H_4 = C_2H_4O + e$	4.05 ± 0.5
$= C_2H_2 + H_2O$	1.9 ± 0.2
$O^- + C_2H_2 = C_2H^- + OH$	8.0 ± 0.5
$= C_2H_2O + e$	13.0 ± 0.9
$= C_2OH^- + H$	0.8 ± 0.1

The reaction with C_2H_4 also produced OH^- , C_2H^- , C_2OH^- and $C_2H_3O^-$ at rates of 0.5 to 10, 5, 1.5 and 2 % respectively of the combined rate of the two major channels.

The upper limits for the rates of the reactions of O_3^- with the same molecules were two orders of magnitude lower.

In an earlier paper,¹ the author described an apparatus for measuring negative ion-molecule reaction rates and gave results for oxygen ion reactions with oxygen molecules. An extension of the use of the drift tube and mass filter to study a wider variety of reactions is achieved by using a slow convective flow system to provide a gas of continuously variable composition. In this particular apparatus with its small diameter photo-cathode and anode there is appreciable radial electron-diffusion. Associative detachment reactions can be differentiated from ordinary ion-molecule reactions by a fall in the anode current which results from the increase in diffusion as the ions revert to electrons. This type of process causes one of the major differences between positive and negative ion-molecule collisions. The molecule plus free electron potential surface may lie in part below that of the ions, possibly opening up another reaction channel, with important effects upon the reaction kinetics.

The associative detachment between O^- and H_2 has been investigated both in the flowing afterglow² and in the drift tube^{3, 4}; the latest results agree within the given error limits. Phelps⁴ has suggested that the reaction should provide a useful standard for thermal ions. Paulson⁵ and Martin and Bailey⁶ have shown, however, that at higher collisional energies in a low-pressure mass spectrometer the reaction to form OH^- is important, but the cross-section for this process is small at the lowest

* present address: Shell Research Ltd., Thornton Research Centre, P.O. Box 1, Chester CH1 3SH.

attainable energies. There is also a strong isotope effect between H_2 and D_2 . Associative detachment would be difficult to follow in such experiments. It is therefore of interest to investigate any isotope effects for thermal ions and to compare the two regimes.

The reactions of the alkanes with O^- , studied in the flowing afterglow⁷ were chosen not only for comparison, but also as a means of changing ion identity and mass to investigate experimental mass discrimination effects.¹

There have been three studies of the $\text{O}^- + \text{C}_2\text{H}_4$ system. In the flowing afterglow Bohme and Young⁸ report a single reaction channel for dissociative attachment, but in low-pressure mass spectrometer experiments Stockdale *et al.*,⁹ and Hughes and Tiernan¹⁰ find appreciable production of C_2H_2^- and OH^- ions. Again dissociative attachment would be difficult to identify in the latter type of experiment, and the interest lies in finding the cause of the differences.

Ion cyclotron resonance investigations of the $\text{O}^- + \text{C}_2\text{H}_2$ reaction have been made by Goode and Jennings.¹¹ The principal products, C_2H^- and C_2OH^- , are the same as those found by Stockdale.⁷

These experiments in oxygen were paralleled by a similar investigation of O^- reaction in carbon dioxide.¹² Comparison of the two systems leads to a fuller description in the latter case and in turn to a better understanding of the apparent radiation chemical stability of CO_2 , which, it is postulated, arises from negative ion back reactions.¹³

EXPERIMENTAL

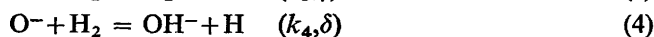
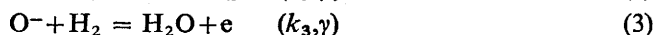
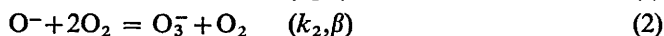
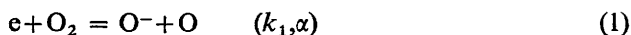
The apparatus has been fully described.¹ It is a drift tube, 80 mm long, from which the ion currents are sampled through a $250\text{ }\mu\text{m}$ hole in the 25 mm diameter anode. They are generated by the attachment of photo-electrons to the gas molecules. The cathode has a diameter of 12 mm. There is a slow convective gas flow through the tube perpendicular to the direction of the drift field.

Results are obtained at a particular pressure and reduced field by following specific ion count rates as a function of reactant concentration. The reactant is added as a minor flow (typically less than 1 %) to the oxygen stream. Gas flows are controlled by needle valves and are measured at atmospheric pressure on calibrated capillary flowmeters. The minor gas pressure is the oxygen pressure multiplied by the flow rate ratio. The total drift tube current to the anode is also recorded. The oxygen was B.O.C. "breathing oxygen". The reactant gases came from the same supplier, except for the deuterium which was supplied by the Matheson Co.

RESULTS

$\text{O}^- + \text{H}_2$; $\text{O}^- + \text{D}_2$

The effect of adding hydrogen to oxygen in the reduced field region between 1 and $5 \times 10^{-16}\text{ V cm}^2\text{ molecule}^{-1}$, where the ions are initially O^- and O_3^- , is to reduce the ion signals. The only product ion is OH^- which reaches a current approximately 5 % of that of the original ions. The anode current falls to a constant value lower than that in O_2 alone. Typical experimental results are shown in fig. 1; the ion currents have been corrected for mass discrimination.¹ Rate constants are obtained by calculating the expected ion signals and comparing these with the observed results. The following model is used with the associated rate constants (k_i) and coefficients ($\alpha - \delta$) given in parentheses.



The rate constants and coefficients are related by the drift velocity of the reactant ion, e.g.,

$$\beta = k_2[\text{O}_2]^2/u \quad (\text{i})$$

where u is the drift velocity of the O^- ion.

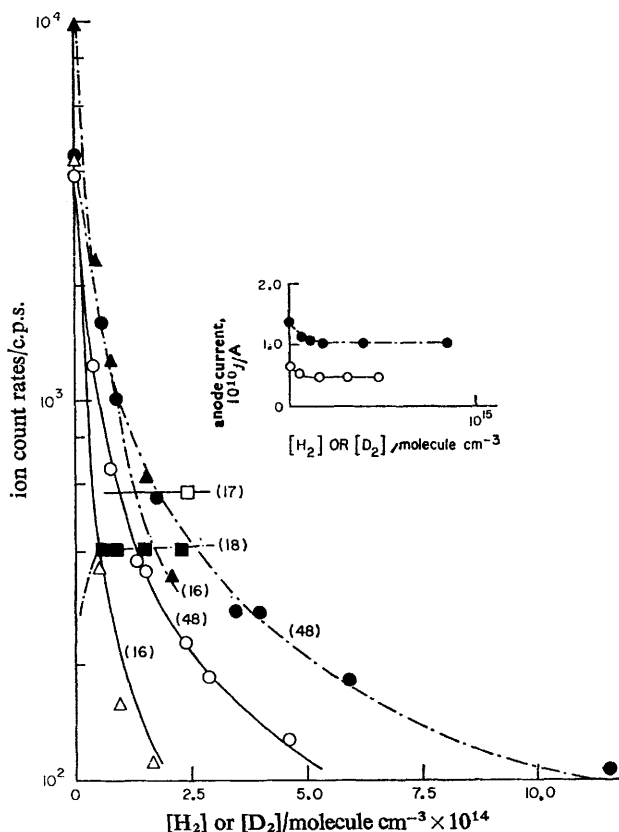


FIG. 1.—Ion count rates and anode current against H_2 or D_2 additions to O_2 . H_2/O_2 , $E/N = 3.9 \times 10^{-16} \text{ V molecule}^{-1} \text{ cm}^{-2}$; O_2 density $= 6.4 \times 10^{16} \text{ molecule cm}^{-3}$. Δ , O^- ; \circ , O_3^- ; \square , OH^- ; solid lines, computations with $k_3 = 7.4 \times 10^{-10}$ and $k_4 = 3.7 \times 10^{-10} \text{ cm}^3 \text{ molecule}^{-1} \text{ s}^{-1}$. D_2/O_2 , $E/N = 4.45 \times 10^{-16}$, O_2 density $= 5.6 \times 10^{16}$; \blacktriangle , O^- ; \bullet , O_3^- ; \blacksquare , OD^- ; dotted lines, computations with $k_5 = 4.3 \times 10^{-10}$ and $k_6 = 1 \times 10^{-11} \text{ cm}^3 \text{ molecule}^{-1} \text{ s}^{-1}$. Insert shows anode current variation: \circ , H_2 addition; \bullet , D_2 .

The total currents, given by j_e for electrons, j_1 for O^- , j_2 for O_3^- and j_3 for OH^- are the solutions of the differential equations:

$$\frac{dj_e}{dx} = -\alpha j_e + \gamma j_1 \quad (\text{ii})$$

$$\frac{dj_1}{dx} = \alpha j_e - (\beta + \gamma + \delta) j_1$$

$$\frac{dj_2}{dx} = \beta j_1$$

$$\frac{dj_3}{dx} = \delta j_1,$$

where x and r are the longitudinal and radial drift tube coordinates. There is significant radial electron diffusion but ion diffusion is negligible. Eqn (ii) must therefore be modified when the solution is sought for the ion current on axis, to which the sampled ion current is proportional. On the assumption that radial and longitudinal diffusion may be treated separately,¹ the equation is

$$\frac{\partial j_e}{\partial x} = -\frac{D}{u} \left(\frac{\partial^2 j_e}{\partial r^2} + \frac{1}{r} \frac{\partial j_e}{\partial r} \right) - \alpha j_e + \gamma j_1, \quad (\text{iii})$$

where D is the diffusion coefficient. The solutions for the ion current on axis are:

$$j_1 = \int_0^L j_0 [1 - \exp(-B/x)] \exp(-\alpha x) \exp(-(\beta + \gamma + \delta)y) \left\{ \sum_{l=1}^{\infty} \frac{\alpha^l (\gamma x y)^{l-1}}{((l-1)!)^2} \right\} dx \quad (\text{iv})$$

$$j_2 = \int_0^L \beta j_{1x} dx \quad (\text{v})$$

$$j_3 = (\delta/\beta) j_2,$$

where $y = L - x$, $B = a^2 E e / 4q$, j_0 is the electron emission current on axis, and j_{1x} is the integral (iv) between the limits 0 and x ; a is the photo-cathode radius, E the applied field, e the electronic charge, L the drift length and q the electron characteristic energy at the particular field, $D/u = q$. The formulae are similar to those given by Frommhold¹⁴ as a solution to a similar problem—the longitudinal spreading of an electron pulse, with detachment and attachment occurring. Each term in the sum under the integral sign represents the current contribution from an ion which has travelled a distance x as an electron and attached l and detached $(l-1)$ times. The probability of a particle going through many such cycles and yet not diffusing away from the axis is small at experimental pressures. Only the first few terms are therefore significant. The calculated currents shown in fig. 1 are the results of computer integration of eqn (iv) and (v). The values taken for α , β , and D are those used or measured before.¹ γ and δ are varied to obtain the fits. The slopes of the O^- and O_3^- curves are sensitive to $(\gamma + \delta)$ but insensitive to β and the OH^-/O_3^- ratio is δ/β . The ion currents are, however, insensitive to α and D . In any given run, the experimental points for all three ion currents can be fitted within curves calculated for γ and δ values which differ by less than 10 %. No variation in the other parameters is allowed. Initial estimates for the two variables are found by considering just the first terms of the series, i.e., by assuming that any detached electrons are lost. In this case the fall in the total ion signal, Δj , is related to the O_3^- signal remaining by:

$$\frac{\Delta j}{j_2} = \frac{(\gamma + \delta)}{\beta} = \frac{(k_3 + k_4)[\text{H}_2]}{k_2[\text{O}_2]^2}.$$

From plots of the ratio against $[\text{H}_2]$, which approximate to straight lines, first estimates for $(\gamma + \delta)$ can be obtained. Similarly one finds:

$$j_3/j_0 = \gamma/(\gamma + \delta)$$

where j_0 is the initial total ion signal. It is found with the present geometry at pressures in the Torr region that the estimates obtained in this way are typically 30 % low. The best fit coefficients were independent of oxygen pressure and reduced field. Furthermore, no reactions of O_3^- with H_2 were necessary to explain the results. The mean rate constants and standard deviations are:

$$k_3 = 7.0 \pm 0.5 \times 10^{-10} \text{ cm}^3 \text{ molecule}^{-1} \text{ s}^{-1}$$

$$k_4 = 0.33 \pm 0.05 \times 10^{-10} \text{ cm}^3 \text{ molecule}^{-1} \text{ s}^{-1}.$$

The O^- mobility has been taken¹⁵ to be $3.2 \text{ cm}^2 \text{ s}^{-1} \text{ V}^{-1}$. The criterion for the effects of longitudinal diffusion to be unimportant is $^1 Ee/kT > \gamma$, where k is Boltzmann's constant and T the effective ion temperature. This is very close to ambient, and the condition becomes $40E > \gamma$ (E is V length^{-1} and γ , length^{-1}), which is easily satisfied by the experimental results. The major uncertainty in the rate comes from the choice between differing values of the ionic drift velocity.

The analysis for deuterium is identical. The reactions are:



with rate constants

$$k_5 = 4.8 \pm 0.5 \times 10^{-10} \text{ cm}^3 \text{ molecule}^{-1} \text{ s}^{-1}$$

$$k_6 = 0.1 \pm 0.02 \times 10^{-10} \text{ cm}^3 \text{ molecule}^{-1} \text{ s}^{-1}.$$

Results of a typical deuterium run are also shown on fig. 1. It is interesting to note that the variations in oxygen ion signal with H_2 or D_2 flowmeter reading are identical, the detachment rate ratio being the same as the viscosity ratio.

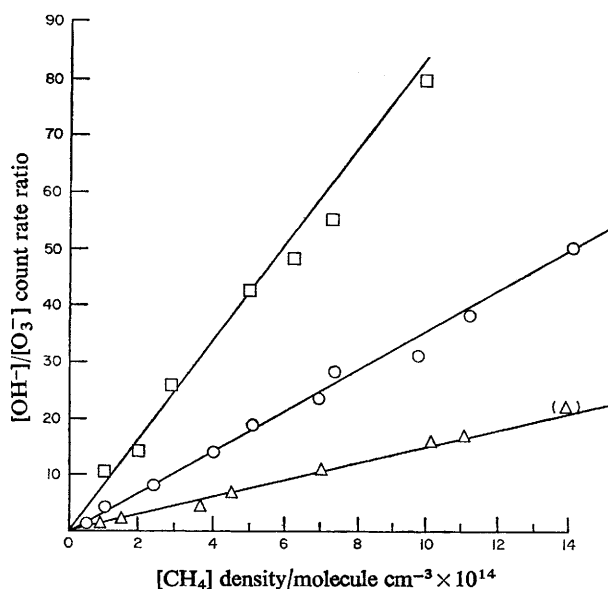
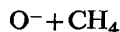
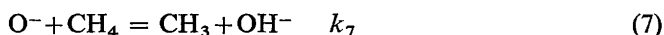


FIG. 2.— OH^-/O_3^- count rate ratio against CH_4 concentration at different O_2 densities. $E/N = 4.15 \times 10^{-16} \text{ V molecule}^{-1} \text{ cm}^{-2}$. Oxygen densities $\times 10^{-16}$ (molecule cm^{-3}): \square , 4.08; \circ , 5.62; \triangle , 7.9 (bracketed point : ratio and density $\times 0.8$).



When methane is added to oxygen, the O^- and O_3^- currents fall but in this case a similar OH^- signal develops. Until sufficient methane is added to change the electron energy and consequently the attachment coefficient, the anode current is unaffected. This suggests a straightforward reaction:



in competition with reaction (2). Irrespective of the spatial distribution of O^- , the

OH^-/O_3^- current ratio equals the rate ratio for their formation, on the assumption that there is no further reaction of either ion, i.e.,

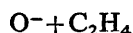
$$j_4/j_2 = k_7[\text{CH}_4]/k_2[\text{O}_2]^2 \quad (\text{vi})$$

where j_4 is the hydroxyl ion signal.

As eqn (vi) predicts, plots of the ratio against CH_4 concentration are straight lines passing through the origin with slope inversely proportional to the square of the oxygen pressure. These lines are shown in fig. 2. The absence of any detectable curvature gives an upper limit for the rate of any reaction of O_3^- with CH_4 of $10^{-13} \text{ cm}^3 \text{ molecule}^{-1} \text{ s}^{-1}$, assuming no OH^- reaction.

The absence of any change in the total drift tube current confirms that there is no associative detachment channel of any significance. The expected constancy of the total ion current was used therefore as the basis of one of the experiments to assess mass discrimination in the measuring system.¹ The rate constant given by the results is $k_2 = 1.1 \pm 0.1 \times 10^{-10} \text{ cm}^3 \text{ molecule s}^{-1}$.

The reaction of ethane was found to be essentially identical but with a high rate constant, in agreement with Bohme.⁷



The product ion spectrum in this case is relatively rich but the total ion current is significantly less than the initial current in oxygen alone. There is a concurrent fall in the anode current confirming that the principal reaction channel is associative detachment,



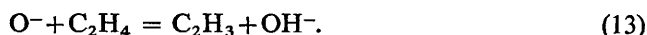
The major ionic product is mass 32; the presence of its expected associates 50 ($\text{O}_2 \cdot \text{H}_2\text{O}^-$) and 64 (O_4^-) confirms it as O_2^- . It must be formed by charge transfer from the initial product ion to O_2 . Low pressure mass spectrometer experiments suggest,⁹ C_2H_2^- .



The other ionic products are a factor of 10 lower in current. They are masses 43, 41 and 25, which it is suggested form a group, and 17 (OH^-). The first three arise from:



The product ratio between these channels is independent of field and pressure; it is $\text{C}_2\text{H}^- : \text{C}_2\text{H}_3\text{O}^- : \text{C}_2\text{HO}^- = 5.0 \pm 1.0 : 2.0 \pm 0.05 : 1.5 \pm 0.5$. The numbers are percentages of the combined rate constant for the major channels (8) and (9). The hydroxyl radical arises by a reaction similar to (7)



The fraction here rises from 0.5 % at a reduced field of $3 \times 10^{-16} \text{ V cm}^2 \text{ molecule}^{-1}$ to 10 % at $8 \times 10^{-16} \text{ V cm}^2 \text{ molecule}^{-1}$.

The results are analyzed in a manner exactly analogous to that used for H_2 and CH_4 . The sum of all the reaction coefficients is found by comparing the observed falls in the O^- and O_3^- currents with calculated curves obtained in the same way as

in the treatment of the hydrogen results. The rate ratio between associative detachment and ion formation is given by a similar comparison in which the product ion current is fitted. The rate for any individual ion-producing reaction is also given by a plot in the form of eqn (vi). A typical experiment with the fitted curves is shown in fig. 3. The following rate constants were obtained for the major channels:

$$k_8 = 4.05 \pm 0.5 \times 10^{-10} \text{ cm}^3 \text{ molecule s}^{-1}$$

$$k_9 = 1.9 \pm 0.2 \times 10^{-10} \text{ cm}^3 \text{ molecule s}^{-1}.$$

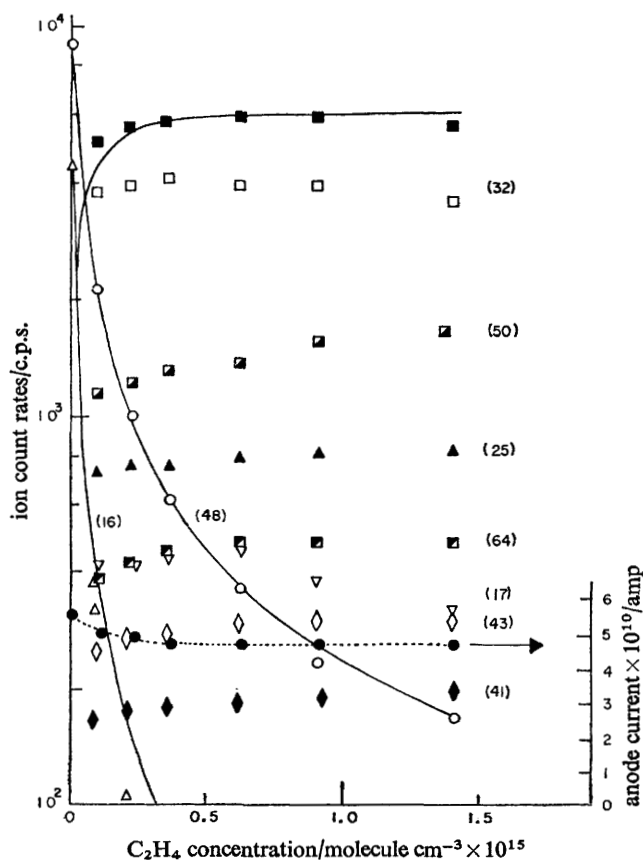
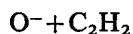


FIG. 3.—Ion count rates and anode current against C_2H_4 concentration. $E/N = 4.2 \times 10^{-16} \text{ V cm}^2 \text{ molecule}^{-1}$, O_2 density $= 9 \times 10^{16} \text{ molecule cm}^{-3}$. Δ , O^- ; \square , O_2^- ; \blacksquare , total O_2^- (\square , mass 32; \blacksquare , 50; \blacksquare , 64) \blacktriangle , C_2H^- ; ∇ , OH^- ; \diamond , $\text{C}_2\text{H}_3\text{O}^-$; \blacklozenge , C_2HO^- . Solid lines are computed with $k_8 = 3.4$, $k_9 = 1.9$, other ions $k = 0.5 \text{ cm}^3 \text{ molecule}^{-1} \text{ s}^{-1} \times 10^{-10}$; \bullet , anode current.

The combined rate constant for ethylene consumption,

$$\sum_{i=8}^{13} k_i = 6.5 \pm 1.0 \times 10^{-10} \text{ cm}^3 \text{ molecule s}^{-1}.$$

The ion fraction appeared to increase by 5 % as the reduced field increased from 2.5 to $4 \times 10^{-16} \text{ V cm}^2 \text{ molecule}^{-1}$ but the overall rate constant remained constant.



The results here are a little simpler. There are just three important reaction channels :

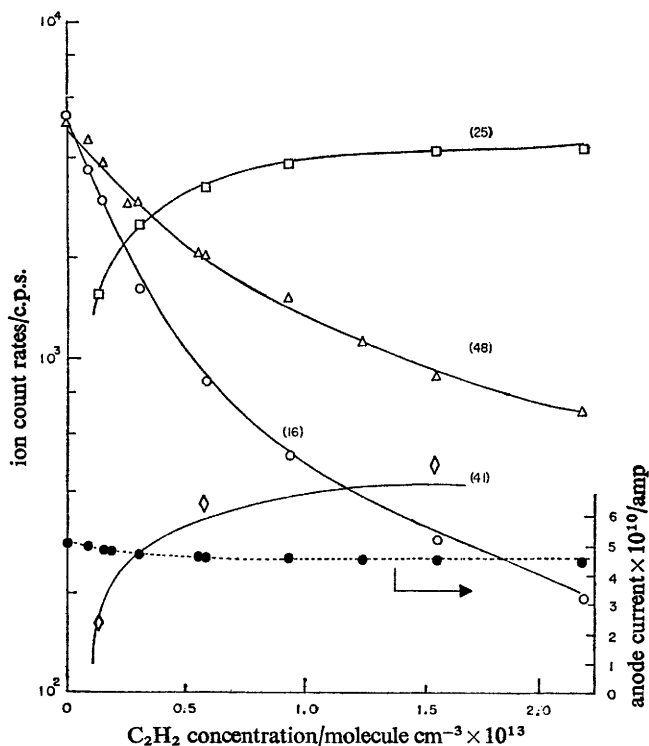


FIG. 4.—Ion count rates and anode current against C_2H_2 concentration. $E/N = 3.35 \times 10^{-16} \text{ V cm}^2 \text{ molecule}^{-1}$, O_2 density $= 5.6 \times 10^{17} \text{ molecule cm}^{-3}$. \circ , O^- ; \triangle , O_3^- ; \square , C_2H^- ; \diamond , C_2HO^- . Solid lines are computed with $k_{14} = 13.5$, $k_{15} = 8.5$, and $k_{16} = 0.85 \text{ cm}^3 \text{ molecule}^{-1} \text{ s}^{-1} \times 10^{-10}$; \bullet , anode current.

Rate constants are obtained from an analysis identical in method to that used for C_2H_4 . Computed curves and experimental points are shown in fig. 4. The following rate constants gave the best fit to the experimental data :

$$\frac{k_{14}}{13.0} \quad \frac{k_{15}}{8.0} \quad \frac{k_{16}}{0.8} \quad (\text{cm}^3 \text{ molecule s}^{-1} \times 10^{-10})$$

Fig. 5 shows plots of the ion current ratio of masses 25/48 against $[\text{C}_2\text{H}_2]$. As anticipated, the presence of an associative detachment channel causes no deviation from linearity. The slopes are again inversely proportional to the square of the oxygen pressure. This will be of importance when comparison is made with the situation in CO_2 .¹² Again there was a small increase in the ion channel rate over the reduced field range but it was less than the significance of the results.

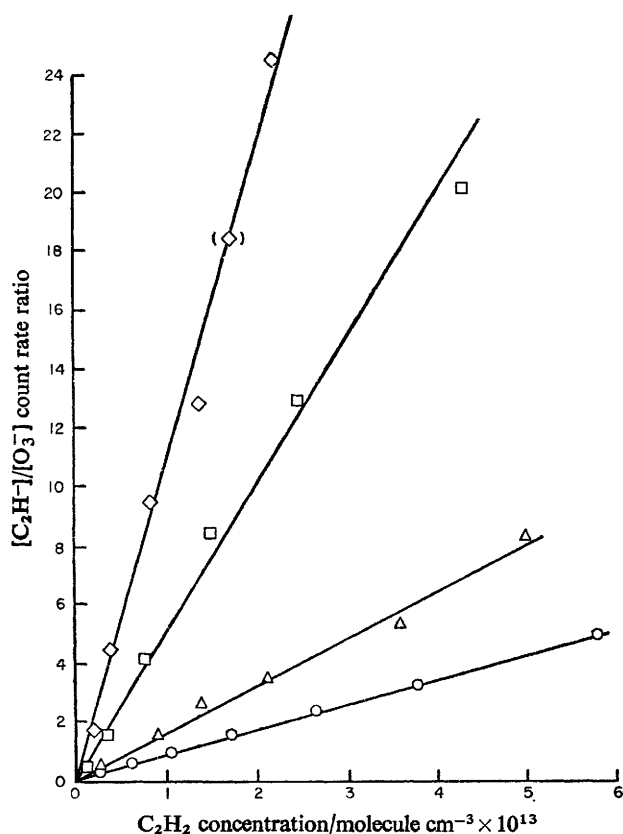
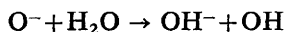


FIG. 5.— $\text{C}_2\text{H}^-/\text{O}_3^-$ count rate ratio against C_2H_2 concentration at different O_2 densities $E/N = 4 \times 10^{-16} \text{ V cm}^2 \text{ molecule}^{-1}$. Oxygen densities $\times 10^{-16} \text{ (molecule cm}^{-3})$ ◇, 3.3; □, 5.7; △, 9.5; ○, 12.7. (Bracketed point: ratio and density $\times 0.5$.)

DISCUSSION



The overall rate constant of $7.0 \times 10^{-10} \text{ cm}^3 \text{ molecule}^{-1} \text{ s}^{-1}$ compares well with the drift tube values of 7.2 obtained by Moruzzi⁴ and his co-workers and the flowing afterglow value of 6.0 by Ferguson² *et al.* Neither of these groups however reported the minor OH^- formation channel. Fehsenfeld¹⁶ did however record an increase in the OH^- signal as H_2 was added to the gas stream in the flowing afterglow but could not differentiate between reaction (4) and



with the H_2O produced by process (3). This cannot be important here because the OH^- current/hydrogen relationship would require a constant $\text{H}_2 : \text{H}_2\text{O}$ ratio, a condition not fulfilled if either the H_2O were produced in sufficient quantity by reaction (3) or if it were present with the O_2 . The measured rate is too high to be explained by H_2O present in the H_2 . Moruzzi,¹⁷ in the experiments with mass identification,³ used a low resolution mass filter which could have obscured an OH^- signal. Both he and Fehsenfeld state that a rate $k_4 \leq 0.05 k_3$ would not be inconsistent with their

results. Gas chromatographic analysis of the hydrogen showed only CH_4 as a significant impurity and this at 10^4 times too low a content to account for the OH^- reaction. The production of OD^- when D_2 was used confirms the reaction. Mass spectrometric analysis of the D_2 indicated no hydrocarbons were present in the reactant above the 20 p.p.m. level.

The ratio of 1.45 ± 0.2 between the hydrogen and deuterium associative detachment rate constants is very close to 1.34, the square root of the reduced mass ratio. This is the expected ratio if the rate is determined by an isotopically independent probability factor, P , multiplying the numbers of ion-induced dipole collisions per second⁴; the rate of such collisions is given by¹⁸:

$$k = 2\pi(\alpha e^2/\mu)^{\frac{1}{2}} \quad (\text{vii})$$

where μ is the reduced mass of the collision partners and α the polarizability of the neutral species.

There is a larger factor, however, between the ion producing rates— 3.5 ± 0.7 —which suggests a change in the probability of emerging from the channel. Associative detachment can occur when the reactants move over a part of the interaction energy surface which lies above that for the molecule and a free electron. If it is assumed that ion production occurs on an upper surface then the overall survival probability into an ionic channel must be calculated to obtain the rate of ion production. Bardsley *et al.*¹⁹ give a formula for the ion production cross section, Q , by dissociative attachment. It is the cross section for attachment, Q_0 , at a internuclear separation, R_0 , in the diatomic case (or reaction coordinate in the more general case) multiplied by the survival probability against detachment as the nuclei separate.

$$Q = Q_0 \exp \left[- \int_{R_0}^R \frac{\Gamma(r)}{\hbar} \frac{dr}{v(r)} \right]$$

where R is the coordinate at which the ion and free electron+molecule surfaces cross, beyond which detachment is forbidden, $\Gamma(r)/\hbar$, the width of the state divided by Planck's constant, is the detachment frequency at (r) and $v(r)$ is the velocity in the r direction. Moruzzi *et al.*⁴ suggest that the associative detachment reaction which is the reverse of dissociative attachment may be treated in a similar manner, and use this hypothesis to explain the fall in rate constant of the $\text{NO} + \text{O}^-$ associative detachment rate with increasing collisional energy. The $\text{O}^- + \text{H}_2$ reaction may be treated in the same way; the probability of a reactive collision producing an ion will be:

$$P_{\text{ion}} = \exp \left[- \frac{R}{\tau} \sqrt{\frac{\mu}{2\varepsilon}} \right] \quad (\text{viii } a)$$

and a free electron

$$P_{\text{det}} = 1 - P_{\text{ion}} \quad (\text{viii } b)$$

where R , τ and ε are averages over all collisional parameters of the length of the reaction coordinate over which detachment may occur, the life time in this region and the energy. Writing $A = R/\tau\sqrt{2\varepsilon}$ and combining eqn (vii) and (viii), then

$$k_4/k_6 = \exp(-A(\sqrt{\mu_1} - \sqrt{\mu_2}))\sqrt{\mu_2}/\sqrt{\mu_1}$$

$$k_3/k_5 = \frac{[1 - \exp(-A\sqrt{\mu_1})]\sqrt{\mu_2}}{[1 - \exp(-A\sqrt{\mu_2})]\sqrt{\mu_1}}$$

The subscript 1 indicates H_2O and 2, D_2O . Using the measured value of $k_4/k_6 = 3.5 \pm 0.7$, together with $\mu_1 = 1.78$ and $\mu_2 = 3.2$ one obtains $A = 2.15 \pm 0.45$ (a.u.)^{-1/2}. This can be used to calculate the ion and electron fraction in either case:

$$\text{H}_2, k_3 : k_4 = 0.94 : 0.06 \pm 0.03 \text{ (cf. experimental, } 0.96 : 0.04)$$

$$\text{D}_2, k_5 : k_6 = 0.98 : 0.02 \pm 0.02 \quad (0.98 : 0.02)$$

The ion fractions and the relative isotope effect are therefore consistent with the model. Furthermore, because detachment is so probable, k_3/k_5 is very close to the inverse reduced mass ratio and the difference between the rates and those of eqn (vii), a factor P of 0.5, must reflect a geometric and statistical weight factor. The value of τ indicated by $A = 2.15$ is not unreasonable; if $R = 10^{-7}$ cm and the mean energy is thermal, $\tau = 10^{-13}$ s. The cross section for ion formation at higher energies can also be predicted, in a semi-quantitative manner, by ignoring any other reaction channels and assuming that τ remains constant. This is equivalent to saying that the reaction coordinate and path across the energy surface are independent of collisional energy. The cross section for ion formation will be:

$$\sigma^2 = 2\pi P \left(\frac{\alpha e^2}{2\varepsilon} \right)^{\frac{1}{2}} \exp \left(-\frac{R \left(\frac{\mu}{2\varepsilon} \right)^{\frac{1}{2}}}{\tau} \right)$$

which in the case of hydrogen is

$$= 6.7 \times 10^{-16} \varepsilon^{-\frac{1}{2}} \exp(-0.57 \varepsilon^{-\frac{1}{2}}) \text{ cm}^2$$

with the energy ε in eV. The detachment cross section is

$$= 6.7 \times 10^{-16} \varepsilon^{-\frac{1}{2}} [1 - \exp(-0.57 \varepsilon^{-\frac{1}{2}})] \text{ cm}^2.$$

For D_2 the exponential factor is $0.76 \varepsilon^{-\frac{1}{2}}$. In fig. 6 the calculated cross sections are compared with the experimental data of Paulson⁵; the latter have been transformed from laboratory to centre-of-mass coordinates. It can be seen that the model predicts the correct value for the isotope effect and shows that the maximum shifts to higher energy for the higher mass. Bailey⁶ has also detected the ion channel and his deuterium results are similar to those of Paulson but his hydrogen cross sections are much lower.

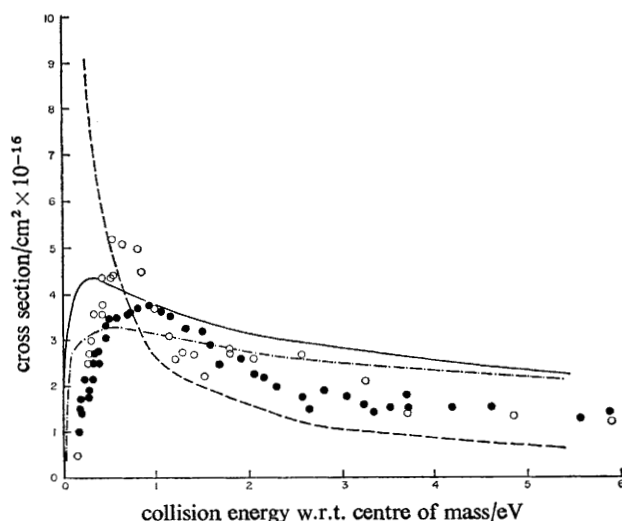
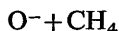


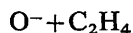
FIG. 6.—Comparison of experimental and calculated cross sections for associative detachment and OH^- formation as a function of collisional energy for O^-/H_2 and D_2 reactions. $\text{O}^- + \text{H}_2 \rightarrow \text{H}_2\text{O} + \text{e}$, calculated — — —; $\text{O}^- + \text{H}_2 \rightarrow \text{OH}^- + \text{H}$, calculated — experimental \circ ; $\text{O}^- + \text{D}_2 \rightarrow \text{OD}^- + \text{D}$, calculated — — — experimental \bullet .

If this model is a generally valid description of negative ion molecule reactions with a detachment channel, one would expect an increase in ion product and a reduction in detachment as collisional energy increases. The present experiments were not conducted over a wide enough field range to test this hypothesis; in the hydrogen case the average collisional energy was only 0.002 eV above thermal at the highest fields.

Claydon, Segal and Taylor²⁰ have recently calculated potential energy surfaces for H_2O^- ; they find the 2A_1 state which correlates with $\text{H}_2(^1\Sigma) + \text{O}^-(^2P)$ and $\text{OH}^-(^1\Sigma) + \text{H}(^2S)$ to be attractive in both dissociation directions. This is consistent with the large overall rate constant, there being no energy barriers.



The measured rate constant of $1.1 \times 10^{-10} \text{ cm}^3 \text{ molecule}^{-1} \text{ s}^{-1}$ is in good agreement with the value of 1.0 measured by Bohme and Fehsenfeld⁷ in the flowing afterglow. This confirms that there is little systematic error between the two methods. No detachment occurs at the experimental energies.

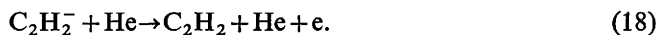


The overall reaction rate of $6.5 \pm 1.0 \times 10^{-10} \text{ cm}^3 \text{ molecule}^{-1} \text{ s}^{-1}$ is in good agreement with the flowing afterglow determination⁸ of 7.6×10^{-10} and the ion production rate is similar to that found in the low pressure mass spectrometric study of Stockdale.⁹ The latter rate does, however, exceed the flowing afterglow upper limit for ion production. The present results were obtained at ion energies very close to thermal and there was little variation in the rates with energy, which suggests that the difference between the earlier results does not arise solely from the different ion energies in the experiments. Although it is possible that some of the minor ion production may arise from impurities, this is not possible for the major products; the minimum gas purity was 99.8%, with the principal impurities in a typical sample ethane 500 p.p.m., ether 300 p.p.m. and methane 250 p.p.m.

The electron affinity of the suggested major ion product C_2H_2^- must obviously be less than that of O_2 , as is required by the charge transfer reaction. In the flowing afterglow the major gas flow is helium, with some oxygen added to give the primary ion O^- . It is suggested ion production could be masked by the charge transfer reaction



and furthermore the detachment reaction (18) may be significant if the electron affinity is low:

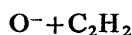


The latter process could destroy all the product ions in the flowing afterglow, but be unable to compete with the excess oxygen in the drift tube. In the low pressure mass spectrometer experiments, the smaller number of collisions can attenuate the effect of (18) even in a more energetic environment. There is an analogous situation in N_2O .²¹ The NO^- formed by the reaction



is detected in the low pressure mass spectrometer but in the drift tube, when N_2O or CO_2 are the major gases, it is almost completely destroyed by detachment. In O_2 , charge transfer eliminates the effect.

The minor ion production rates are not greater than the flowing afterglow upper limits, and it is suggested that the low energy experiments can be brought into line by considering reactions (17) and (18) in the flowing afterglow. The greater importance of the ionic channel at low energy in this and the case of acetylene compared with that of H_2 must arise from lower transition probabilities to detachment. The slower moving, heavier particles would be expected to form fewer ions if the lifetimes in eqn (viii) were similar. Again, ion formation should become dominant at higher energy, but the increase in rate constant will be much less. As the ion/detachment rate ratio ≈ 0.5 for near thermal ions eqn (viii) would predict a $C_2H_2^+$ formation rate of $6 \times 10^{-10} \text{ cm}^3 \text{ molecule}^{-1} \text{ s}^{-1}$ in the eV region. This compares well with Stockdale's upper limit of 4.2 ± 1.3 , but is significantly lower than Hughes' 3×10^{-9} at 0.3 eV. These two report OH^- fractions of $\frac{1}{7}$ and $\frac{1}{4}$ respectively. The rise to such a value from 1/200 at 0.04 eV shows that the simple model is not sufficient to describe all the observed features.



The rate for ion production is in good agreement with that measured by low pressure mass spectrometry.⁹ The value of $2.0 \times 10^{-9} \text{ cm}^3 \text{ molecule}^{-1} \text{ s}^{-1}$ in the eV region correlates well with 0.8×10^{-9} for 40 % ion formation at thermal energies. The rate constant from the ion cyclotron resonance experiments, 4×10^{-10} , is significantly lower. There is little disagreement, however, between the methods on the relative importance of the C_2H^- and C_2OH^- channels. It is not clear whether any of the techniques other than the drift tube could have detected associative detachment. The low pressure mass spectrometric experiments could not establish whether OH^- was a product because the background was high—these experiments show that it was not formed more than 10^{-3} times as frequently as C_2H^- .

When the overall rate of associative detachment plus ion formation is taken, it exceeds the expected upper limit from eqn (vii). This equation can be re-expressed in terms of the dielectric constant ϵ of the neutral species to give a rate expression.

$$k = 12.8 \times 10^{-10} \{(\epsilon - 1) \times 10^4 / \mu\}^{\frac{1}{2}} \quad (\text{ix})$$

where μ is now in a.u. (atomic units).

If 1.001 34 is taken as the dielectric constant of acetylene at N.T.P.,²²

$$k = 1.48 \times 10^{-9} \text{ cm}^3 \text{ molecule}^{-1} \text{ s}^{-1}.$$

This is significantly less than 2.2×10^{-9} , the total overall rate, which suggests that the long-range interaction potential is more attractive than the assumed charge-induced dipole.

Hyatt and Stanton²³ have investigated theoretically the importance of multipole potentials in ion-linear molecule collisions. They find that the quadrupole moment in the cases they consider ($Ar^+ - H_2$, $H_2^+ - N_2$) causes some deviation from the Langevin model at low energy (0.1 eV). Acetylene has a relatively high quadrupole moment²⁴ ($1.1 \times 10^{-16} \text{ e}$). An order of magnitude estimate of its effect may be calculated, if a spherically symmetrical average interaction potential is assumed²⁵:

$$\phi_q = \frac{1}{20 kT} \frac{e^2 Q^2}{r^6} = 7.6 \times 10^{-58} / r^6$$

where Q is the quadrupole moment, and r is measured in cm. This modifies the charge induced dipole potential:

$$\phi_d = -e^2 \alpha / 2r^4 = -4.56 \times 10^{-43} / r^4.$$

The result is an increase of approximately 5 % in the impact parameter or 10 % in the cross section for collisions of thermal energy. Although this is less than the difference between the observed and the charge-induced dipole cross sections, it is indicative of the importance of the extra term. It should be noted that the unaveraged ϕ_q is a r^{-3} interaction multiplied by an angular term and it will be dominant at favoured angles. A more detailed analysis is necessary to ascertain the full quantitative effect, but this simple approach suggests that the extra interaction may be sufficient to explain the large cross sections and rate constants.

The usefulness of a drift tube and slow convective flow system to measure negative ion-molecule reaction rates has been demonstrated. The results agree well overall with those obtained by other methods, although evidence for more reaction channels has been found in several cases.

It is suggested that the variation in ion production with collisional energy in several negative ion-molecule reactions may be described in terms of a competition between detachment and ion production. This predicts that at high energies ion production will be dominant with detachment important at low energy. This can be tested by extending the field range of the drift tube experiments.

The author thanks the U.K.A.E.A. for a Research Fellowship and Dr. C. B. Amphlett for his encouragement. He also thanks Dr. J. L. J. Rosenfeld for his helpful suggestions, Drs. J. L. Moruzzi and F. C. Fehsenfeld for their communications, and Dr. J. F. Paulson for permission to quote his unpublished results.

¹ D. A. Parkes, *Trans. Faraday Soc.*, 1971, **67**, 711.

² E. E. Ferguson, F. C. Fehsenfeld and A. L. Schmeltekopf, *Adv. Chem.*, 1969, **80**, 83.

³ J. L. Moruzzi and A. V. Phelps, *J. Chem. Phys.*, 1966, **45**, 4617.

⁴ J. L. Moruzzi, J. W. Eakin and A. V. Phelps, *J. Chem. Phys.*, 1968, **48**, 3070.

⁵ J. F. Paulson, unpublished results.

⁶ J. D. Martin and T. L. Bailey, *J. Chem. Phys.*, 1968, **49**, 1977.

⁷ D. K. Bohme and F. C. Fehsenfeld, *Can. J. Chem.*, 1969, **47**, 2715.

⁸ D. K. Bohme and L. B. Young, *J. Amer. Chem. Soc.*, 1970, **92**, 3301.

⁹ J. A. D. Stockdale, R. N. Compton and P. W. Reinhardt, *Int. J. Mass Spectr. Ion Phys.*, 1970, **4**, 401.

¹⁰ B. M. Hughes and T. O. Tiernan, personal communication cited in ref. (8).

¹¹ C. G. Goode and K. A. Jennings, to be published.

¹² D. A. Parkes, *J.C.S. Faraday I*, 1972, **68**, 627.

¹³ A. R. Anderson and D. A. Dominey, *Rad. Res. Rev.*, 1968, **1**, 269.

¹⁴ L. Frömmhold, *Fort. Phys.*, 1964, **12**, 597.

¹⁵ R. M. Snuggs, D. J. Volz, J. H. Shummers, D. W. Martin and E. W. McDaniel, *Phys. Rev. A.*, 1971, **3**, 477.

¹⁶ F. C. Fehsenfeld, personal communication.

¹⁷ J. L. Moruzzi, personal communication.

¹⁸ G. Gioumouis and P. D. Stevenson, *J. Chem. Phys.*, 1958, **29**, 294.

¹⁹ J. N. Bardsley, A. Herzenberg and F. Mandl, *Proc. Phys. Soc.*, 1966, **89**, 321.

²⁰ C. R. Claydon, G. A. Segal and H. S. Taylor, *J. Chem. Phys.*, 1971, **54**, 3799.

²¹ D. A. Parkes, to be published.

²² E. C. Gregg, Jr., *Handbook of Chemistry and Physics*, ed. R. C. Weast (The Chemical Rubber Co., Cleveland, 1968), p. E62.

²³ D. Hyatt and L. Stanton, *Proc. Roy. Soc. A*, 1970, **318**, 107.

²⁴ R. M. Hill and W. V. Smith, *Phys. Rev.*, 1951, **82**, 451.

²⁵ J. O. Hirschfelder, C. F. Curtiss and R. R. Bird, *Molecular Theory of Gases and Liquids* (Wiley, New York, 1954), pp. 27, 28.